CMOS-Free Magnetic Domain Wall Leaky Integrate-and-Fire Neurons with Intrinsic Lateral Inhibition

Naimul Hassan[1], Wesley H. Brigner[1], Xuan Hu[1], Otitoaleke G. Akinola[2], Christopher H. Bennett[3], Matthew J. Marinella[3], Felipe Garcia-Sanchez[4,5], Jean Anne C. Incorvia[2], Joseph S. Friedman[1]

[1]Department of Electrical and Computer Engineering, The University of Texas at Dallas, Richardson, TX USA
[2]Department of Electrical and Computer Engineering, The University of Texas at Austin, Austin, TX USA
[3]Sandia National Laboraties, Alburquerque, NM USA
[4]Departamento de Física Aplicada, Universidad de Salamanca, Salamanca, Spain
[5]Istituto Nazionale di Ricerca Metrologica, Torino, Italy

***Abstract*—Spintronic devices, especially those based on motion of a domain wall (DW) through a ferromagnetic track, have received a significant amount of interest in the field of neuromorphic computing because of their non-volatility and intrinsic current integration capabilities. Many spintronic neurons using this technology have already been proposed, but they also require external circuitry or additional device layers to implement other important neuronal behaviors. Therefore, they result in an increase in fabrication complexity and/or energy consumption. In this work, we discuss three neurons that implement these functions without the use of additional circuitry or material layers.**

Keywords*—*Artificial neuron, leaky integrate-and-fire (LIF) neuron, magnetic domain wall (DW), neural network crossbar, neuromorphic computing, three-terminal magnetic tunnel junction (3T-MTJ)

I. Introduction

Modern von Neumann computers are able to efficiently solve problems of staggering proportions assuming a well-structured input, but are considerably less efficient at solving real-world problems with unstructured data sets. In fact, the human brain can significantly outperform classical computers in terms of both speed and efficiency when solving such unstructured problems [1]-[3]. Therefore, a considerable amount of effort has been devoted to replicating the human brain in the form of a circuit.

According to neuroscientists, the human brain consists of two primary components – neurons and synapses. Neurons are comprised of axons (cell bodies), which originate electrical signals depending on inputs from other neurons, and dendrites, which allow the signals from the axons to propagate to other neurons. Synapses, on the other hand, are electrically conductive components that bridge the gap between the dendrites of one neuron and the axon of others. To replicate these components, researchers have developed artificial neuron and synapse analogs. Synapses have already been implemented using an assortment of technologies, including, but not limited to, memristors [4], magnetic skyrmion devices [5], three-terminal magnetic tunnel junctions (3T-MTJs) [6], [7], and even organic devices [8]. However, owing to the complexity of neurons, fewer spintronic neurons have been developed [9], [10]. To resolve this issue, we have developed three neurons based on the 3T-MTJ [11]-[13], which are discussed in this work. Section II provides a brief background in the subjects of spintronics and neuromorphic computing. Sections III-V provide details on the aforementioned neurons, followed by conclusions in Section VI.

II. Background

A. Neural Network Crossbar Array

An NxM neural network crossbar array consists of N input neurons and M output neurons. By convention, the input neurons are connected to inputs of the horizontal wires (word lines), and the output neurons are connected to the outputs of the vertical wires (bit lines). The synapses connect the word and bit lines and provide the weighting between the input and output neurons [14].

B. Leaky Integrate-and-Fire Neuron

Initially, researchers developed what is known as an integrate-and-fire (IF) neuron. Recently, however, an improvement on the IF neuron known as the leaky integrate-and-fire (LIF) neuron emerged. This neuron performs three primary functionalities – integrating, where the neuron accepts a current input and increases the stored energy accordingly; leaking, where no input is applied and the stored energy gradually decreases; and firing, where the neuron quickly releases the stored energy as an output spike and resets itself. The state of the neuron can be represented as a voltage stored on a capacitor or the position of a domain wall (DW) within a ferromagnetic track.

C. Three Terminal Magnetic Tunnel Junction

A typical magnetic tunnel junction (MTJ) is comprised of a free ferromagnetic layer whose magnetization can be switched using external stimuli, generally a current, magnetic field, or a combination of the two. This free layer is separated from another fixed layer whose magnetization state cannot be switched by a thin insulating tunnel barrier. When a current is passed through the free layer, it is polarized in the same direction of the free layer's magnetization. As the current then flows through the fixed layer, the fixed layer will re-polarize the current in its own direction, thereby inhibiting the current flow if the two states are not parallel to each other. Therefore, by altering the magnetization of the free layer, it is possible to

978-1-7281-3320-1/20/$31.00 ©2020 IEEE

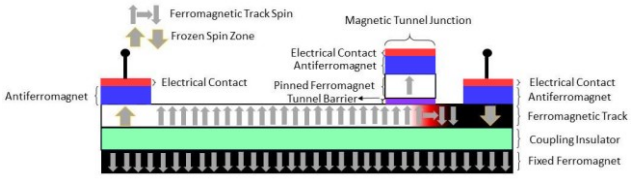

Fig. 1. 3T-MTJ with fixed ferromagnet underneath. The magnetic field applied by the fixed ferromagnet on the bottom will cause the DW (shown in red) to move from right to left.

change the resistance between the low resistance state (LRS) when the magnetizations are parallel and the high resistance state (HRS) when the magnetizations are antiparallel.

A 3T-MTJ is a modification of the MTJ where the free layer is stretched and contains two antiparallel magnetic domains instead of just one. A DW provides a smooth transition between the two domains. If electron flow is passed through one domain into the other, the current is polarized in the same direction as the initial domain it passes through. When it reaches the second domain, the electron flow is inhibited by the same effect described above. However, since both domains exist in the free layer, the current also has an effect on the second domain and gradually polarizes the second domain in the same direction as the first. This causes the first domain to expand and the second to shrink, thereby shifting the DW [15], [16]. This mechanism is called spin transfer torque (STT). By shifting the DW from one side of the track to the other, the magnetization state under the fixed layer can be switched between being parallel and antiparallel to that of the fixed layer, thereby facilitating changes in the resistance state of the device. Due to the fact that, without any external excitation, DWs can remain in one position for long periods of time, they have garnered significant interest in a number of fields where non-volatility is highly desirable, particularly neuromorphic computing [16]-[18].

III. Intrinsically Leaking 3T-MTJ Device with Dipolar Coupling Field

One of the methods we proposed to implement intrinsic leaking uses a dipolar coupling field produced by an electrically isolated ferromagnet underneath the DW track. As discussed in this section, this will cause the DW to leak from one side of the track to the other without any external excitation.

A. Device Structure

The device is virtually identical to the 3T-MTJ structure described above. However, it contains an electrically isolated ferromagnet situated beneath the DW track, which is used to apply a dipolar coupling field to the track. The structure is displayed in Figure 1.

The functionality of the device was verified using MuMax3 [19], which is a micromagnetic simulator. The DW track was 600 nm long, 32 nm wide, and 1 nm thick. In MuMax3, the track was comprised of 1x1x1 nm^3 cells. To prevent the DW from annihilating itself on the ends of the track, two 30-nm-wide antiferromagnets were placed on top of the DW track, one on each side. This effectively pinned the magnetization states, and provided the DW with a 540 nm range of motion along the DW track. The magnetic saturation M_{sat} was 1 T, the exchange stiffness A_{ex} was $1.3*10^{-11}$ J/m, the perpendicular anisotropy constant k_{u1} is $4*10^5$ J/m^3, the nonadiabaticity factor ξ is 0.9, the Landau-Lifshitz-Gilbert damping constant α is 0.015, and the polarization of spin transfer torque is 1.

B. Leaking with Dipolar Coupling Field

When a magnetic field parallel to one of the domains in a DW track is applied to the track, the domain parallel to the field will tend to expand and the domain antiparallel to the field will tend to shrink. Using this mechanism, it is possible to create an effective energy landscape more favorable to the DW existing on one side of the track than the other. This causes the DW to shift along the track from right to left.

C. Combined Integrating and Leaking with Dipolar Coupling Field

However, when a current is applied from right to left through the track, the resulting electron flow will cause the DW to shift from left to right through the track using STT. Due to the energy landscape produced by the magnetic field, shifting the DW to a higher energy state using a current effectively stores energy in the form of the DW's position along the track. Figure 2 demonstrates the combined integrating and leaking functionalities. A pulse train consisting of three 2 ns pulses is applied to the track. Each pulse is followed by a 30 ns leaking period, where the DW is allowed to leak in the absence of an excitation current.

D. Firing through Magnetoresistance Switching

Assuming the neuron fires whenever the DW passes underneath the MTJ, switching the device from HRS to LRS, the device will produce an output current spike and reset the DW to the original position. Additionally, the device will not integrate any input current pulses for a brief period – called the refractory period – after firing.

IV. Intrinsically Leaking 3T-MTJ Device with Graded Anisotropy

This section discusses the use of an anisotropy gradient, which can be implemented using either Ga^+ ion irradiation of the DW track or the fabrication of a TaO_x wedge on top of the track. Again, this will cause the DW to leak without the use of any external circuitry.

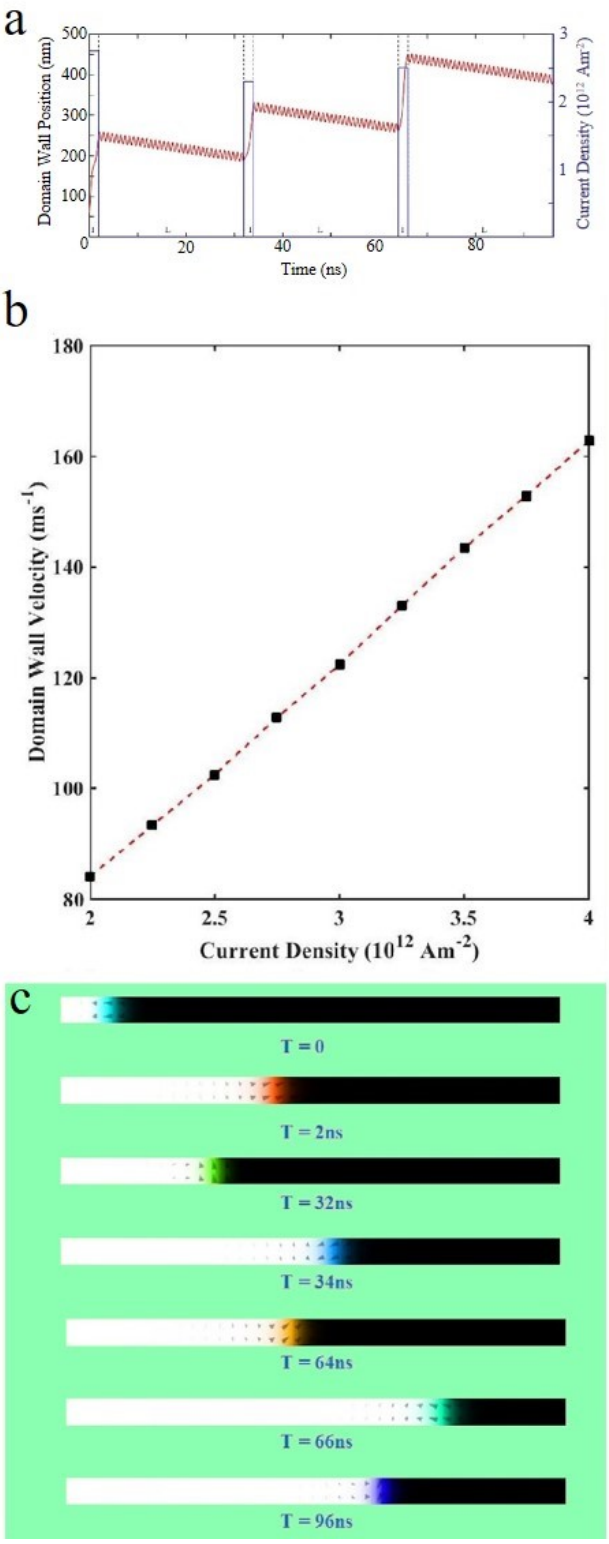

Fig. 2. (a) DW position and current density vs time demonstrating combined integrating and leaking functionalities. Each 2 ns integration period is followed by a 30 ns leaking period where no input is applied resulting in a 96 ns total runtime. (b) Average DW velocity vs current density. As the current density increases, the integration speed increases as well. (c) Snapshots of the micromagnetic simulation for time t =0 ns, t = 2 ns, t = 32 ns, t = 34 ns, t = 64 ns, t = 66 ns, and t = 96 ns. Note that the DW magnetization state rotates – this is evidence of DW precession.

As with the previous neuron, the device structure is virtually identical to a normal 3T-MTJ device. Instead of using a dipolar coupling field to implement the leaking, the device uses a linear anisotropy gradient. The DW track is 250 nm long, 32 nm wide, and 1.5 nm thick, and the MuMax3 cell size is 1x1x1.5 nm^3. Additionally, the antiferromagnets on either end of the track are 10 nm wide, allowing for a 230 nm range of motion for the DW. The exchange stiffness A_{ex} is $1.3*10^{-1}$ J/m, the Landau-Lifshitz-Gilbert damping constant α is 0.02, the nonadiabiticity of spin transfer torque ξ is 0.2, and the magnetic saturation M_{sat} is $800*10^3$ A/m, or approximately 1 T. The lower magnetocrystalline anisotropy value $anis_l$ is $5*10^5$ J/m^3, and the upper magnetocrystalline anisotropy value $anis_h$ is $5*10^6$ J/m^3. Since no external excitation is applied, the magnetic field B_{ext} is 0 T.

B. *Leaking with Graded Anisotropy*

In general, a DW tends to have a lower energy when it exists in a low anisotropy ferromagnet and a higher energy when it exists in a high anisotropy ferromagnet. As such, a linearly graded anisotropy will provide an energy landscape that is more favorable to the DW existing in the lower anisotropy regions of the track than in the higher anisotropy regions of the track. This allows the DW to shift along the track without the use of any external excitation.

C. *Combined Integrating and Leaking with Graded Anisotropy*

Similar to the neuron with a dipolar coupling field, the energy landscape produced by the graded anisotropy allows for energy accumulation by using STT to shift the DW to the higher-anisotropy regions of the track. The combined integrating and leaking functionalities of the device are demonstrated in Figure 3. A current pulse train with 2 ns wide current pulses is applied to the input of the device; however, each pulse is followed by a 50 ns leaking period instead of a 30 ns leaking period.

D. *Firing through Magnetoresistance Switching*

Again, this neuron fires when the DW passes underneath the fixed layer and the device state switches from the HRS to

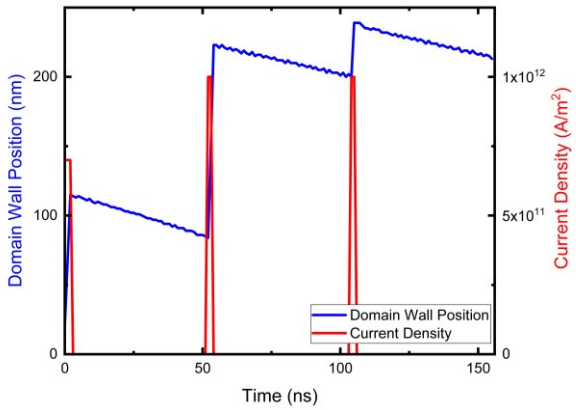

Fig. 3. DW position and current density vs time demonstrating the combined leaking and integrating functionalities of a 3T-MTJ neuron with graded anisotropy. Each 2 ns-wide current pulse is followed by a 50 ns leaking period, resulting in a 156 ns runtime.

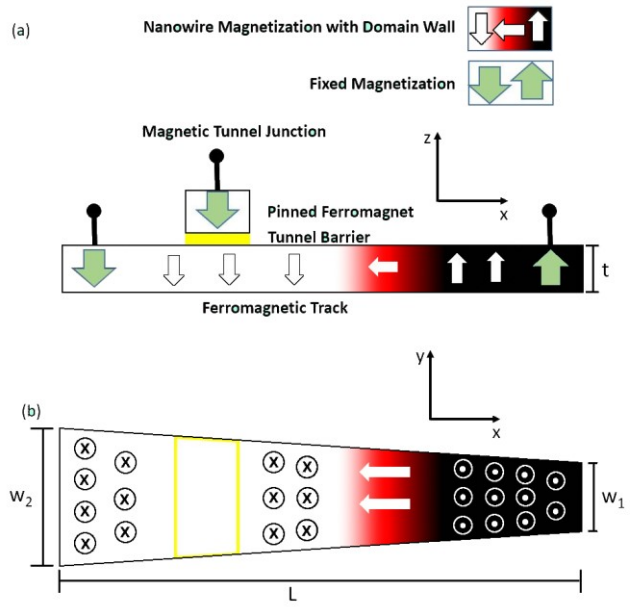

Fig. 4. (a) Side view of the device. (b) Top view of the device, demonstrating the trapezoidal x-y cross-section.

the LRS. The neuron then resets itself and enforces a brief refractory period.

V. Intrinsically Leaking 3T-MTJ Device with Shape-Based DW Drift

Finally, in this section, we discuss the use of shape variations of the DW track to implement intrinsic leaking. Although the mechanism behind this phenomenon, known as shape-based domain wall drift (SDD), is different than the mechanisms behind the other two leaking methods, this device is still fully capable of leaking without any external excitations.

A. Device Structure

Unlike the previous two neurons, this neuron does not maintain the rectangular x-y cross-section of the 3T-MTJ. Instead, it exhibits a trapezoidal x-y cross-section, as illustrated in Figure 4.

The DW track is 250 nm long and 1.5 nm thick. At its narrowest, the DW track is 25 nm wide, and at its widest, the DW track is 100 nm wide. As with the neuron with graded anisotropy, the antiferromagnets on either end of the track are 10 nm wide and the DW has a 230 nm range of motion. The material parameters of the track represent CoFeB [20], where the exchange stiffness A_{ex} is 1.3 * 10^{-11} J/m, the Landau-Lifshitz-Gilbert damping constant α is 0.02, the nonadiabaticity of spin-transfer torque ξ is 0.2, and the magnetic saturation M_{sat} is 1 T.

B. Leaking with Shape-Based DW Drift

A DW tends to exist in a lower energy state in a narrower track than in a wider track. Similar to the previous two neurons, the aforementioned shape variation will result in an energy landscape more favorable to the DW existing in one region of the track than in others. If a current is used to shift the DW to a wider region of the track, the DW will consequently shift to the narrower regions of the track when the current is removed.

C. Firing through Magnetoresistance Switching

As with the previous two neurons, the device fires once the DW has passed underneath the fixed ferromagnet. The DW is reset to the original position, and the device exhibits a brief refractory period where no input currents are provided to the neuron.

VI. Conclusions

Three neurons able to intrinsically provide the leaking, integrating, and firing capabilities required of LIF neurons are discussed in this work. These devices were implemented using dipolar coupling fields, anisotropy gradients, or cross-sectional variations – all of which are modifications of common 3T-MTJ devices. These novel neurons can reduce the external circuitry required to implement neural networks, which, in turn, can reduce the fabrication complexity and power consumption of this powerful computing paradigm. As a result, the neurons discussed in this work could be significant in the development of future neural network systems.

Acknowledgments

This research is sponsored in part by the National Science Foundation under CCF awards 1910800 and 1910997. The authors thank E. Laws, J. McConnell, N. Nazir, L. Philoon, and C. Simmons for technical support, and the Texas Advanced Computing Center at The University of Texas at Austin for providing computational resources. Sandia National Laboratories is a multimission laboratory managed and operated by NTESS, LLC, a wholly owned subsidiary of Honeywell International Inc., for the U.S. Department of Energy's National Nuclear Security Administration under contract DE-NA0003525. This paper describes objective technical results and analysis. Any subjective views or opinions that might be expressed in the paper do not necessarily represent the views of the U.S. Department of Energy or the United States Government.

References

[1] V. Balasubramanian, "Heterogeneity and Efficiency in the Brain," *Proceedings of the IEEE* 103(8), 1346-1358 (2015).

[2] F. Akopyan, *et al.*, "TrueNorth: Design and Tool Flow of a 65 mW 1 Million Neuron Programmable Neurosynaptic Chip," *IEEE Transactions on Computer-Aided Design of Integrated Circuits and Systems* 34(10), 1537-1557 (2015).

[3] P. A. Merolla, *et al.*, "A million spiking-neuron integrated circuit with a scalable communication network and interface," *Science* 345(6197), 668-673 (2014).

[4] D. B. Strukov, G. S. Snider, D. R. Stewart, R. S. Williams, "The missing memristor found," *Nature* 453(7191), 80-83 (2008).

[5] X. Chen, *et al.*, "A compact skyrmionic leaky-integrate-fire spiking neuron device," *Nanoscale* 10(13), 6139-6146 (2018).

[6] S. Dutta, S. A. Siddiqui, F. Buttner, L. Liu, C. A. Ross, M. A. Baldo, "A logic-in-memory design with 3-terminal magnetic tunnel junction function evaluators for convolutional neural networks," *IEEE/ACM*

International Symposium on Nanoscale Architectures (NANOARCH) (2017).

[7] O. Akinola, E. J. Kim, N. Hassan, J. S. Friedman, J. A. C. Incorvia, "Neuromorphic Computing with Domain Wall-Based Three-Terminal Magnetic Tunnel Junctions: Synapse, " *Joint IEEE International Magnetics Conference & Conference on Magnetism and Magnetic Materials*, Jan. 2019.

[8] Y. V. D. Burgt, *et al.*, "A non-volatile organic electrochemical device as a low-voltage artificial synapse for neuromorphic computing," *Nature Materials* 16(4), 414-418 (2017).

[9] S. Li, W. Kang, Y. Huang, X. Zhang, Y. Zhou, W. Zhao, "Magnetic skyrmion-based artificial neuron device," *Nanotechnology* 28, 31LT01 (2017).

[10] D. Zhang, L. Zeng, K. Cao, M. Wang, S. Peng, Y. Zhang, Y. Zhang, J. O. Klein, Y. Wang, W. Zhao, "All spin artificial neural networks based on compound spintronic synapse and neuron," *IEEE Trans. Biomed. Circuits Syst.* 10, 828 (2016).

[11] N. Hassan, X. Hu, L. Jiang-Wei, W. H. Brigner, O. G., Akinola, F. Garcia-Sanchez, M. Pasquale, C. H. Bennett, J. A. C. Incorvia, J. S. Friedman, "Magnetic domain wall neuron with lateral inhibition," *Journal of Applied Physics* 124(15), 152127 (2018).

[12] W. H. Brigner, X. Hu, N. Hassan, C. H. Bennett, J. A. C. Incorvia, F. Garcia-Sanchez, J. S. Friedman, "Graded-Anisotropy-Induced Magnetic Domain Wall Drift for an Artificial Spintronic Leaky Integrate-and-Fire Neuron," *IEEE Journal on Exploratory Solid-State Computational Devices and Circuits*, 5(1), 19-24 (2019).

[13] W. H. Brigner, N. Hassan, L. Jiang-Wei, X. Hu, D. Saha, C. H. Bennett, M. J. Marinella, J. A. C. Incorvia, F. Garcia-Sanchez, J. S. Friedman, "Shape-Based Magnetic Domain Wall Drift for an Artificial Spintronic Leaky Integrate-and-Fire Neuron," *IEEE Transacations on Electron Devices* 66(11), 4970-4975 (2019).

[14] C. H. Bennett, J. A. C. Incorvia, X. Hu, N. Hassan, J. S. Friedman, M. M. Marinella, "Semi-Supervised Learning and Inference in Domain-Wall Magnetic Tunnel Junction (DW-MTJ) neural Networks," *Proc. SPIE Spintronics XII*, Aug. 2019 (invited).

[15] Currivan, J. A., Jang, Y., Mascaro, M. D., Baldo, M. A., Ross, C. A., "Low Energy Magnetic Domain Wall Logic in Short, Narrow, Ferromagnetic Wires," *IEEE Magnetics Letters* 3, 3000104-3000104 (2012).

[16] Currivan-Incorvia, J. A., Siddiqui, S., Dutta, S., Evarts, E. R., Ross, C. A., Baldo, M. A., "Spintronic logic circuit and device prototypes utilizing domain walls in ferromagnetic wires with tunnel junction readout," *IEEE International Electron Devices Meeting (IEDM)* (2015).

[17] J. S. Friedman, A. V. Sahakian, "Complementary Magnetic Tunnel Junction Logic," *IEEE Transactions on Electron Devices* 61(4), 1207-1210 (2014)

[18] X. Hu, A. Timm, W. H. Brigner, J. A. C. Incorvia, J. S. Friedman, SPICE-Only Model for Spin-Transfer Torque Domain Wall MTJ Logic, *IEEE Transactions on Electron Devices*, 66(6), 2817-2821 (2019).

[19] Vansteenkiste, A., Leliaert, J., Dvornik, M., Helsen, M., Garcia-Sanchez, F., Waeyenberge, B. V., "The design and verification of MuMax3," *AIP Advances* 4(10), 107133 (2014).

[20] Y. Zhang *et al.*, "Compact Modeling of Perpendicular-Anisotropy CoFeB/MgO Magnetic Tunnel Junctions," *IEEE Transactions on Electron Devices* 59(3), 819-826 (2012)